Properties of Organometallic Sulfur-Rich Dithiolate Complexes $[M(L)(C_8H_4S_8)]$ (M = Rh^{III} and Ir^{III}; L = η^5-C_5H_5 and η^5-C_5Me_5) and Their Oxidation

Kazuhiro Kawabata,[a] Motohiro Nakano,[a] Hatsue Tamura,[a] and Gen-etsu Matsubayashi*[a]

Keywords: Electrical conductivity / EPR spectroscopy / Iridium / Oxidation / Rhodium / S ligands / X-ray diffraction

$[Rh(\eta^5\text{-}C_5H_5)(C_8H_4S_8)]$ and $[M(\eta^5\text{-}C_5Me_5)(C_8H_4S_8)]$ [M = Rh^{III} and Ir^{III}. $C_8H_4S_8^{2-}$ = 2-{(4,5-ethylenedithio)-1,3-dithiole-2-ylidene}-1,3-dithiole-4,5-dithiolate(2–)] were prepared by reactions of $[NMe_4]_2[C_8H_4S_8]$ with $[Rh(\eta^5\text{-}C_5H_5)Cl_2]_2$ or $[M(\eta^5\text{-}C_5Me_5)Cl_2]_2$ (M = Rh and Ir). They exhibit oxidation potentials of between +0.16 and +0.24 V (versus Ag/Ag$^+$) with oxidation of the dithiolate ligand. The geometries and electronic states of their one-electron-oxidized species $[M(L)(C_8H_4S_8)]^+$ and $[RhX(L)(C_8H_4S_8)]$ (M = Rh and Ir; X = Br and I; L = η^5-C_5H_5 and η^5-C_5Me_5), obtained by reactions of the above complexes with bromine, iodine, or the ferrocenium cation are discussed based on their ESR spectra. The oxidized η^5-C_5Me_5-metal complexes exhibit electrical conductivities of between 10^{-6} and 10^{-4} S cm^{-1}, while some oxidized η^5-C_5H_5-Rh complexes show conductivities of between 10^{-3} and 10^{-2} S cm^{-1} measured for compacted pellets at room temperature. The X-ray crystal structures of the two-electron-oxidized species $[MI(\eta^5\text{-}C_5Me_5)(C_8H_4S_8)](I_3)$ (M = Rh and Ir) were also clarified.

Introduction

Metal complexes with the sulfur-rich dithiolate ligands $C_3S_5^{2-}$ [4,5-disulfanyl-1,3-dithiole-2-thiolate(2−)] and $C_8H_4S_8^{2-}$ [2-{(4,5-ethylenedithio)-1,3-dithiole-2-ylidene}-1,3-dithiole-4,5-dithionate(2−)] have attracted much attention because the oxidized species exhibit unusual electrical and magnetic properties.[1−4] In particular, the oxidized $C_8H_4S_8$-metal complexes often form effective electron-conduction pathways through several sulfur-sulfur non-bonding contacts in the solid state, resulting in the formation of good electrical conductors. Although planar metal complexes are generally efficient for molecular packing in the solid state, non-planar $C_8H_4S_8$-metal complexes may also form a unique molecular packing with some sulfur-sulfur non-bonding contacts in the solid state and are expected to exhibit new physical properties.

From this standpoint, oxidized cyclopentadienyl- and pentamethylcyclopentadienyl-metal complexes with sulfur-rich dithiolate ligands as non-planar species are of much interest. In our previous studies we reported the related C_3S_5-Co^{III} [5] and -Rh^{III} complexes[6] and some non-planar cyclopentadienyl-metal complexes with the $C_8H_4S_8$ ligand exhibiting high electrical conductivities.[7−9]

[a] Department of Applied Chemistry and Frontier Research Center, Graduate School of Engineering, Osaka University 1−16, Machikaneyama, Toyonaka, Osaka 560−0043, Japan
E-mail: matsu@ch.wani.osaka-u.ac.jp

This paper reports the preparation and properties of $[Rh(\eta^5\text{-}C_5H_5)(C_8H_4S_8)]$ and $[M(\eta^5\text{-}C_5Me_5)(C_8H_4S_8)]$ (M = Rh and Ir) and their oxidation. Furthermore, the geometries and electronic states of their one-electron-oxidized species $[M(L)(C_8H_4S_8)]^+$ and $[RhX(L)(C_8H_4S_8)]$ (M = Rh and Ir; X = Br and I; L = η^5-C_5H_5 and η^5-C_5Me_5), obtained by reaction of the above complexes with bromine, iodine, or the ferrocenium cation, are discussed based on their ESR spectra. The electrical conductivities of the one-electron- and further electron-oxidized species obtained, together with X-ray crystal structures of $[MI(\eta^5\text{-}C_5Me_5)(C_8H_4S_8)](I_3)$ [M = Rh^{III} and Ir^{III}], are also described.

Results and Discussion

Electrochemical Properties of $[Rh(\eta^5\text{-}C_5H_5)(C_8H_4S_8)]$ (1), $[Rh(\eta^5\text{-}C_5Me_5)(C_8H_4S_8)]$ (2) and $[Ir(\eta^5\text{-}C_5Me_5)(C_8H_4S_8)]$ (3)

Figure 1 shows the cyclic voltammogram of complex **2** measured in dichloromethane. The coupled oxidation/reduction peak potentials at +0.15/+0.05 V and at +0.55/+0.45 V (versus Ag/Ag$^+$) are ascribed to the almost reversible processes of the $[Rh(\eta^5\text{-}C_5Me_5)(C_8H_4S_8)]$/$[Rh(\eta^5\text{-}C_5Me_5)(C_8H_4S_8)]^+$ and $[Rh(\eta^5\text{-}C_5Me_5)(C_8H_4S_8)]^+$/$[Rh(\eta^5\text{-}C_5Me_5)(C_8H_4S_8)]^{2+}$ species, respectively. These oxidation peak potentials are lower than those (+0.55 and +0.66 V) of the corresponding complex $[Rh(\eta^5\text{-}C_5Me_5)(C_3S_5)]$,[6] since many $C_8H_4S_8$-metal complexes exhibit somewhat lower oxidation potentials than the corresponding C_3S_5-metal complexes.[4,7–11] The oxidation occurs essentially on the sulfur-rich dithiolate ligand, as observed for other metal complexes with $C_8H_4S_8^{2-}$ [4,7–9] or $C_6S_8R_2^{2-}$ (R = long alkyl chains) dithiolate ligands.[12]

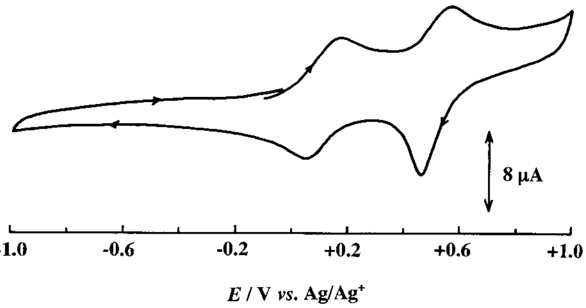

Figure 1. Cyclic voltammogram of complex **2** (1.0×10^{-3} mol·dm^{-3}) in dichloromethane; supporting electrolyte, 0.1 mol·dm^{-3} [N*n*Bu$_4$][ClO$_4$]; sweep rate 500 mV s^{-1}

Complex **1** exhibits somewhat higher oxidation potentials (+0.20 and +0.71 V versus Ag/Ag$^+$) than those of **2**. This finding is ascribed to the more electron-releasing property of the η^5-C_5Me_5 group, as observed for other η^5-C_5H_5- and η^5-C_5Me_5-metal complexes with the $C_8H_4S_8$ ligand [M = Co^{III},[7] Ti^{IV} and Zr^{IV} [8,9]].

The oxidation potentials (+0.44 and +0.65 V versus Ag/Ag$^+$) of the η^5-C_5Me_5-Ir^{III} complex **3** are somewhat higher than those of the corresponding η^5-C_5Me_5-Rh^{III} complex **2**, as has also been observed for the related C_3S_5-metal complexes: [Rh(η^5-C_5Me_5)(C_3S_5)], +0.45 and 0.73 V;[6] [Ir(η^5-C_5Me_5)(C_3S_5)], +0.54 and +0.78 V (versus Ag/Ag$^+$).[13]

Thus, complexes **1–3** can be oxidized by bromine, iodine and the ferrocenium ion.

Oxidation of Complexes 1–3

The electronic absorption spectra of complex **2** in dichloromethane in the presence of varying amounts of iodine as an oxidizing agent are shown in Figure 2. Addition of excess amounts of the oxidant gives the final spectrum of the two-electron-oxidized species [RhI(η^5-C_5Me_5)($C_8H_4S_8$)]$^+$, as described below. The band at 700 nm due to the intramolecular charge transfer (CT) transition from the η^5-C_5Me_5 group to the Rh^{III} ion/$C_8H_4S_8$ ligand moiety[7] is shifted to the region around 1100 nm. Upon addition of iodine a broad band ascribed to the one-electron-oxidized species appears initially at around 1200 nm and finally the strong band due to the two-electron-oxidized species appears at 1040 nm. Addition of bromine to **2** in dichloromethane also affords similar bands due to the oxidized species. For the oxidation of the Ir^{III} complex **3** similar bands due to the one- and two-electron-oxidized species occur at 1050–1200 nm.

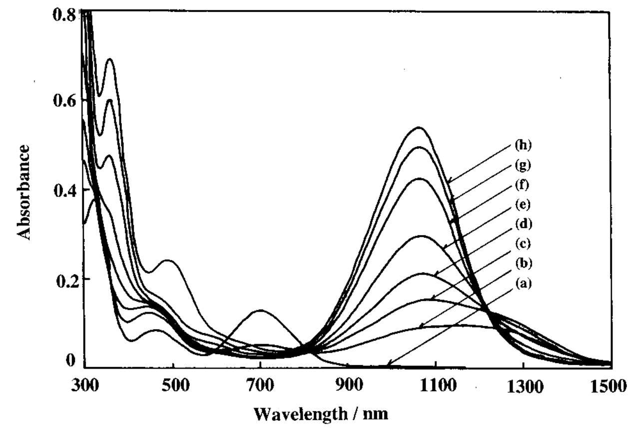

Figure 2. Electronic absorption spectra of complex **2** (2.0×10^{-5} mol·dm^{-3}) in dichloromethane in the presence of iodine; concentration of iodine (mol·dm^{-3}): (a) 0, (b) 0.6×10^{-5}, (c) 1.0×10^{-5}, (d) 1.4×10^{-5}, (e) 2.0×10^{-5}, (f) 3.0×10^{-5}. (g) 4.0×10^{-5}, (h) 2.0×10^{-4}

The reaction of **1** with bromine or iodine gives the one-electron-oxidized species [Rh(η^5-C_5H_5)($C_8H_4S_8$)](Br) (**4**), [Rh(η^5-C_5H_5)($C_8H_4S_8$)](I) (**6**) and [Rh(η^5-C_5H_5)($C_8H_4S_8$)]($I_{4.2}$) (**7**). The oxidized species **7** obtained by the reaction with an excess amount of iodine contains formally the 4.2I$^-$ ion, actually made up from approximately equimolar amounts of both the I_3^- and I_5^- ions, as confirmed by the Raman spectrum, which exhibits bands at 114 and 166 cm^{-1} ascribed to the I_3^- and I_5^- ions, respectively.[14,15] Oxidation reactions of **2** with bromine, iodine or [Fe(η^5-C_5H_5)$_2$][PF$_6$] gave the one-electron-oxidized complexes [RhBr(η^5-C_5Me_5)($C_8H_4S_8$)] (**5**), [RhI(η^5-C_5Me_5)($C_8H_4S_8$)] (**9**), [Rh(η^5-C_5Me_5)($C_8H_4S_8$)][PF$_6$] (**13**), and the two-electron-oxidized species [RhI(η^5-C_5Me_5)($C_8H_4S_8$)](I_3) (**10**). Similarly, complex **3** was oxidized to afford the one-electron-oxidized species [IrBr(η^5-C_5Me_5)($C_8H_4S_8$)] (**6**), [IrI(η^5-C_5Me_5)($C_8H_4S_8$)] (**11**), [Ir(η^5-C_5Me_5)($C_8H_4S_8$)][PF$_6$] (**14**), and the two-electron-oxidized complex [IrI(η^5-C_5Me_5)($C_8H_4S_8$)](I_3) (**12**). The presence of M–X bonds (M = Rh and Ir; X = Br and I) in the oxidized complexes **5**, **6**, **9** and **11** was confirmed by the ESR spectra, as described below.

ESR Spectra of the Oxidized Species

Figure 3 shows the ESR spectra of the one-electron-oxidized species [RhBr(η^5-C_5Me_5)($C_8H_4S_8$)] (**5**) and [Rh(η^5-C_5Me_5)($C_8H_4S_8$)][PF$_6$] (**13**) dissolved in dichloromethane at room temperature. Complex **13** shows an intense, sharp isotropic signal at g = 2.009 (peak-to-peak line width, 0.51 mT). This is ascribed to the radical species of the oxidized $C_8H_4S_8$ ligand moiety, as observed for other oxidized $C_8H_4S_8$-metal [Co^{III},[7] Ti^{IV},[8] Pt^{II},[10] V^{IV} and Mo^{IV},[11] and Au^{III} [16]] complexes with a dithiolate ligand-centered oxidation. The one-electron-oxidized Ir^{III} analog **14** also exhibits a sharp ESR signal at g = 2.009 (peak-to-peak line width, 0.49 mT). Both these complexes in the solid state have shown a somewhat broad isotropic signal at g = 2.008 (peak-to-peak line width, 6.0–7.0 mT).

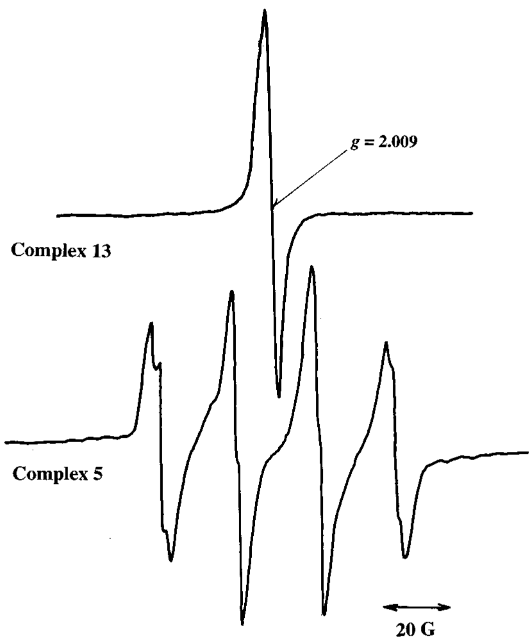

Figure 3. ESR spectra of one-electron-oxidized complexes **5** and **13** in dichloromethane at room temperature

Complex **5** shows an isotropic signal at $g = 2.007$ which consists of a doublet (^{103}Rh, $I = 1/2$) of quadruplets [^{79}Br (50.54%) and ^{81}Br (49.46%), $I = 3/2$]; the ^{103}Rh and $^{79/81}$Br hyperfine couplings are 0.27×10^{-3} and 2.1×10^{-3} cm^{-1}, respectively. This confirms the Rh−Br bond for the oxidized species in solution. These small hyperfine coupling values indicate much lower spin-densities on the metal and bromine atoms, which is very similar to the cases of [RhBr(η^5-C_5Me_5)(C_3S_5)][6] and [CoBr(η^5-C_5Me_5)(C_3S_5)].[5] For the present complex, a one-electron oxidation also occurs at the $C_8H_4S_8$ ligand moiety, as confirmed by the Mulliken spin densities calculated for [RhBr(η^5-C_5Me_5)(C_3S_5)][6] and [CoBr(η^5-C_5Me_5)(C_3S_5)].[5] The ^{103}Rh and $^{79/81}$Br hyperfine couplings for the present complex are appreciably smaller than those (0.47×10^{-3} and 3.0×10^{-3} cm^{-1}, respectively) of [RhBr(η^5-C_5Me_5)(C_3S_5)],[6] suggesting the delocalization of more spin density onto the $C_8H_4S_8$ ligand.

Figure 4 shows the ESR spectra of a dichloromethane solution of [Rh(η^5-C_5Me_5)($C_8H_4S_8$)] in the presence of varying amounts of iodine. [RhI(η^5-C_5Me_5)($C_8H_4S_8$)] is formed in solution (Figure 4a), as indicated by an isotropic signal coupled with the ^{127}I ($I = 5/2$) nucleus [hyperfine coupling, 3.3×10^{-3} cm^{-1}]. The spectrum of isolated [RhI(η^5-C_5Me_5)($C_8H_4S_8$)] (**9**) is the same as that shown in Figure 4a. Upon further addition of iodine to the solution (Figure 4b and 4c) the intensity of the signal is weakened, since the amount of the diamagnetic two-electron-oxidized species is increased. In the presence of an excess amount of iodine (Figure 4d), the signal essentially disappears, with the presence of a very small amount of the one-electron-oxidized species [Rh(η^5-C_5Me_5)($C_8H_4S_8$)]$^+$. The two-electron-oxidized species [RhI(η^5-C_5Me_5)($C_8H_4S_8$)](I_3) (**10**) was obtained by the reaction of **2** with excess amounts of iodine and its crystal structure determined, as discussed below.

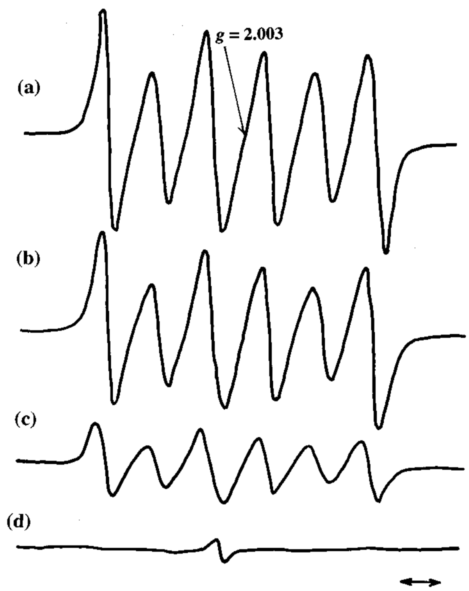

Figure 4. ESR spectra of complex **2** (5.0×10^{-4} mol·dm^{-3}) in dichloromethane in the presence of varying amounts of iodine; concentration of iodine (mol·dm^{-3}): (a) 2.5×10^{-4}, (b) 3.5×10^{-4}, (c) 5.0×10^{-4}, (d) 2.0×10^{-4}

Oxidation of the Ir^{III} analog **3** by the reaction with bromine or iodine yielded both [IrX(η^5-C_5Me_5)($C_8H_4S_8$)] (X = Br and I) and [Ir(η^5-C_5Me_5)($C_8H_4S_8$)]$^+$ as one-electron-oxidized species. Figure 5 shows the ESR spectra of the one-electron-oxidized complex [IrI(η^5-C_5Me_5)($C_8H_4S_8$)] (**11**) dissolved in dichloromethane and in the solid state. The spectrum in solution consists of a sharp signal of [Ir(η^5-C_5Me_5)($C_8H_4S_8$)]$^+$ and a sextet for [IrI(η^5-C_5Me_5)($C_8H_4S_8$)] due to coupling with the ^{127}I nucleus, indicating that the complex consists of both the oxidized species. The solid-state spectrum also shows signals due to both species.

Oxidation of [Rh(η^5-C_5H_5)($C_8H_4S_8$)] (**1**) with bromine or iodine affords essentially the oxidized species without Rh−Br and Rh−I bonds. The ESR spectra of these oxidized species **4**, **6** and **7** show a sharp isotropic signal at $g =$ 2.006−2.008. They are one-electron-oxidized species with a $C_8H_4S_8$ ligand-centered oxidation.

X-ray Crystal Structures of [RhI(η^5-C_5Me_5)($C_8H_4S_8$)](I_3) (10) and [IrI(η^5-C_5Me_5)($C_8H_4S_8$)](I_3) (12)

The crystal structure of **10** consists of three independent molecules which have very similar geometries. This also occurs for **12**. The molecular structure of one of the three cation moieties of **10** is shown in Figure 6, together with the atom-labeling scheme. Selected bond lengths and angles relevant to the $C_8H_4S_8$-Rh moieties of **10**, as well as those of **12**, are listed in Table 1. The Rh(1) atom is bonded to one η^5-C_5Me_5 subunit with Rh−C distances of 2.180−2.218 Å [Rh(2)−C: 2.157−2.201; Rh(3)−C:

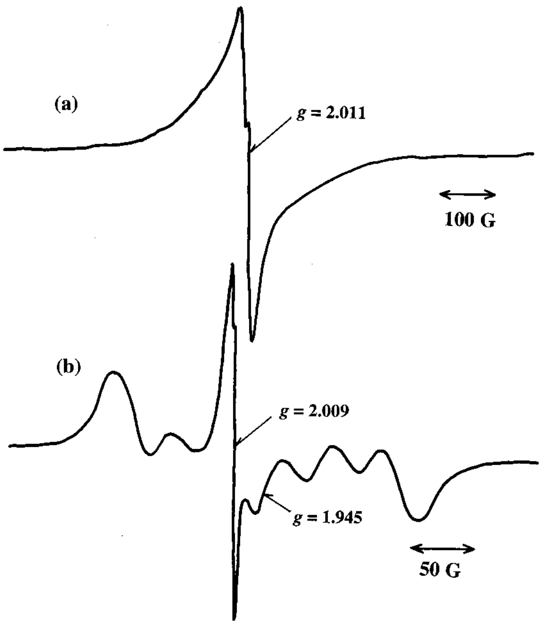

Figure 5. ESR spectra of complex **11** in the solid state (a) and in dichloromethane (b)

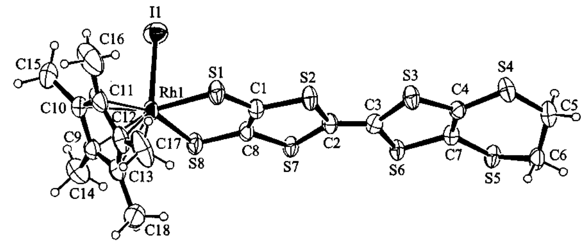

Figure 6. Molecular geometry of one of the cation moieties of complex **10** together with the atom-labeling scheme

2.153−2.204 Å] and to the bidentate chelating dithiolate ligand with Rh(1)−S(1) and −S(8) bonds of 2.326(1) and 2.346(2) Å, respectively, [Rh(2)−S(9) and −S(16): 2.355(2) and 2.308(2) Å; Rh(3)−S(17) and −S(24): 2.328(2) and 2.300(2) Å], which, together with the Rh−I bond, give a formally hexacoordinate geometry. This is close to the geometry of [CoBr(η^5-C_5Me_5)(C_3S_5)].[5] The Rh−S distances are similar to those of related η^5-C_5Me_5-Rh^{III} dithiolate complexes, such as [Rh(η^5-C_5Me_5)(C_3S_5)]$_2$ (2.3571, 2.3774 Å),[6] [Rh(η^5-C_5Me_5){$S_2C_2(CN)_2$}] (2.345, 2.346 Å)[17] and [Rh(η^5-C_5Me_5){$S_2C_2(CN)_2$}]$_2$ (2.350, 2.351 A).[18] The Rh−I distances [2.6854(7), 2.6932(7), 2.7001(5) Å] are also close to that [2.709(1) Å] of [RhI(COEt)(PPh_3){$S_2C_2(CN)_2$}].[19] For the coordinating $C_8H_4S_8$ ligand, the dihedral angle between the Rh(1)−S(1)−S(8) plane and the S(1)−C(1)−C(8)−S(8) plane is 5.72°, and the $C_8H_4S_8$ moiety is almost planar (±0.07 Å). This is also the case for the Rh(2) and Rh(3) moieties. These findings are similar to those of other oxidized $C_8H_4S_8$-metal complexes with a $C_8H_4S_8$ ligand-centered oxidation — [Pt(bpy)($C_8H_4S_8$)][BF_4] (bpy = 2,2′-bipyridine)[20] and [Au(ppy)($C_8H_4S_8$)]$_2$[PF_6] [ppy$^-$ = *C*-deprotonated-2-phenylpyridine(−)][21] — but are in great contrast to the characteristic folding of the TiS_2C_2 plane along the S(1)−S(8) axis, by 35.9°, observed for [Ti(η^5-C_5Me_5)$_2$($C_8H_4S_8$)].[8] The Ir−I, Ir−S and Ir−C bond lengths of **12** are also very close to those of the corresponding Rh−I, Rh−S and Rh−C bonds of **10**.

The crystal structure of **10** is illustrated in Figure 7. Between the three non-equivalent [RhI(η^5-C_5Me_5)($C_8H_4S_8$)]$^+$ cation moieties there are many S−S non-bonding contacts (< 3.7 Å; 3.518−3.662 Å) (19 S···S contacts in a unit cell), together with many other S···I contacts (< 4.0 Å;

Table 1. Relevant bond lengths (Å) and angles (°) for complexes **10** and **12**

	10 (M = Rh)	**12** (M = Ir)
M(1)−I(1)	2.6932(7)	2.703(1)
M(2)−I(2)	2.7001(5)	2.703(1)
M(3)−I(3)	2.6854(7)	2.690(1)
M(1)−S(1-1)	2.326(1)	2.312(3)
M(1)−S(8-1)	2.346(2)	2.325(3)
M(2)−S(1-2)	2.355(2)	2.338(3)
M(2)−S(8-2)	2.308(2)	2.297(3)
M(3)−S(1-3)	2.328(2)	2.319(3)
M(3)−S(8-3)	2.300(2)	2.296(3)
M(1)−C(C_5Me_5, mean)	2.190	2.20
M(2)−C(C_5Me_5, mean)	2.185	2.20
M(3)−C(C_5Me_5, mean)	2.186	2.19
S(1-1)−C(1-1)	1.683(6)	1.68(1)
S(1-2)−C(1-2)	1.684(6)	1.69(1)
S(1-3)−C(1-3)	1.675(6)	1.68(1)
S(8-1)−C(8-1)	1.678(5)	1.682(9)
S(8-2)−C(8-2)	1.684(5)	1.684(10)
S(8-3)−C(8-3)	1.687(5)	1.684(9)
C(1-1)−C(8-1)	1.411(8)	1.42(2)
C(1-2)−C(8-2)	1.417(9)	1.41(2)
C(1-3)−C(8-3)	1.413(9)	1.40(2)
C(2-1)−C(3-1)	1.373(8)	1.37(1)
C(2-2)−C(3-2)	1.378(7)	1.39(1)
C(2-3)−C(3-3)	1.384(7)	1.39(1)
I(1)−M(1)−S(1-1)	89.23(5)	88.45(8)
I(2)−M(2)−S(1-2)	92.04(5)	90.96(9)
I(3)−M(3)−S(1-3)	89.41(4)	88.77(7)
I(1)−M(1)−S(8-1)	88.59(5)	88.25(8)
I(2)−M(2)−S(8-2)	89.53(5)	89.06(9)
I(3)−M(3)−S(8-3)	87.00(4)	86.76(8)
S(1-1)−M(1)−S(8-1)	87.13(5)	86.89(9)
S(1-2)−M(2)−S(8-2)	87.20(6)	87.0(1)
S(1-3)−M(3)−S(8-3)	87.88(6)	87.5(1)
M(1)−S(1-1)−C(1-1)	104.0(2)	104.9(3)
M(2)−S(1-2)−C(1-2)	103.2(2)	103.9(4)
M(3)−S(1-3)−C(1-3)	102.8(2)	103.4(4)
M(1)−S(8-1)−C(8-1)	103.4(2)	104.3(4)
M(2)−S(8-2)−C(8-2)	104.8(2)	105.2(4)
M(3)−S(8-3)−C(8-3)	104.4(2)	104.6(4)
S(1-1)−C(1-1)−C(8-1)	122.3(4)	121.6(7)
S(1-2)−C(1-2)−C(8-2)	122.7(4)	121.9(7)
S(1-3)−C(1-3)−C(8-3)	123.7(4)	123.0(7)
S(8-1)−C(8-1)−C(1-1)	122.8(4)	121.9(7)
S(8-2)−C(8-2)−C(1-2)	121.8(4)	121.8(8)
S(8-3)−C(8-3)−C(1-3)	120.9(4)	121.2(8)

3.648−3.989 Å) (27 S···I contacts in a unit cell) between the $C_8H_4S_8$ moieties and the I_3^- ions, which results in the formation of a two-dimensional molecular array along the *a* and *b* axes. These molecular arrays are separated by both the η^5-C_5Me_5 moieties and the I_3^- ions along the *c* axis. Complex **12** has essentially the same crystal structure as that of **10**.

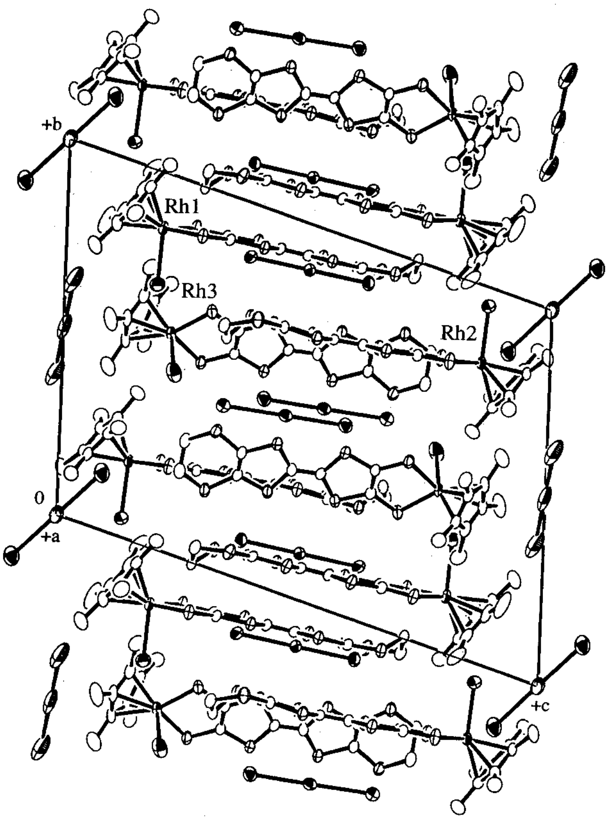

Figure 7. Packing diagram of complex **10**

Electrical Conductivities of the Oxidized Complexes

The electrical conductivities of the oxidized complexes measured for compacted pellets at room temperature are listed in Table 2.

Table 2. Electrical conductivities (σ) of the oxidized complexes[a]

Complex[a]	σ_{RT} (S cm^{-1})
$[Rh(\eta^5\text{-}C_5H_5)(C_8H_4S_8)](Br)$ (**4**)	6.5×10^{-3}
$[Rh(\eta^5\text{-}C_5H_5)(C_8H_4S_8)](I)$ (**7**)	2.5×10^{-2}
$[Rh(\eta^5\text{-}C_5H_5)(C_8H_4S_8)](I_{4.2})$ (**8**)	7.6×10^{-5}
$[RhBr(\eta^5\text{-}C_5Me_5)(C_8H_4S_8)]$ (**5**)	6.1×10^{-6}
$[RhI(\eta^5\text{-}C_5Me_5)(C_8H_4S_8)]$ (**9**)	2.0×10^{-4}
$[RhI(\eta^5\text{-}C_5Me_5)(C_8H_4S_8)](I_3)$ (**10**)	1.2×10^{-5}
$[RhI(\eta^5\text{-}C_5Me_5)(C_8H_4S_8)][PF_6]$ (**13**)	2.4×10^{-6}
$[IrBr(\eta^5\text{-}C_5Me_5)(C_8H_4S_8)]$ (**6**)	3.0×10^{-6}
$[IrI(\eta^5\text{-}C_5Me_5)(C_8H_4S_8)]$ (**11**)	1.1×10^{-6}
$[IrI(\eta^5\text{-}C_5Me_5)(C_8H_4S_8)](I_3)$ (**12**)	5.0×10^{-6}
$[IrI(\eta^5\text{-}C_5Me_5)(C_8H_4S_8)][PF_6]$ (**14**)	$< 10^{-7}$

[a] Measured for compacted pellets at room temperature.

The conductivities of the one-electron-oxidized η^5-C_5Me_5-Rh^{III} and -Ir^{III} complexes are very low. This seems essentially to come from an inadequate molecular packing in the solid state, which results in ineffective S−S nonbonding interactions between the oxidized $C_8H_4S_8$ ligand moieties. On the other hand, the one-electron-oxidized η^5-C_5H_5-Rh^{III} species **4** and **7** exhibit considerably higher electrical conductivities. These species without Rh−X (X = Br and I) bonds seem to have a more effective molecular packing through S···S interactions. These packing modes may be similar to those of the $[Co(\eta^5\text{-}C_5H_5)(C_8H_4S_8)]^+$ species, which also exhibits high electrical conductivity.[7] The present study also shows the effectiveness of the $C_8H_4S_8$ ligand for the construction of an electron conduction pathway even for non-planar metal complexes.

Experimental Section

Materials: $[Rh(\eta^5\text{-}C_5H_5)Cl_2]_2$,[22] $[Rh(\eta^5\text{-}C_5Me_5)Cl_2]_2$ [22,23] and $C_8H_4S_8(CH_2CH_2CN)_2$,[10,24,25] as a pro-ligand for the $C_8H_4S_8^{2-}$ dithiolate ligand, as well as $[Fe(\eta^5\text{-}C_5Me_5)_2][PF_6]$,[26] were prepared according to the literature procedures.

Preparation of $[Rh(\eta^5\text{-}C_5H_5)(C_8H_4S_8)]$ (1), $[Rh(\eta^5\text{-}C_5Me_5)(C_8H_4S_8)]$ (2) and $[Ir(\eta^5\text{-}C_5Me_5)(C_8H_4S_8)]$ (3): All the following reactions were performed under an argon atmosphere. A methanol (0.48 mL) solution of NMe_4OH (120 mg, 1.3 mmol) was added with vigorous stirring to a tetrahydrofuran (50 mL) solution of $C_8H_4S_8(CH_2CH_2CN)_2$ (190 mg, 0.42 mmol) and the mixture was stirred for 15 min. The resulting red brown $[NMe_4]_2[C_8H_4S_8]$ was filtered, and dissolved in ethanol (50 mL). A dichloromethane (20 mL) solution of $[Rh(\eta^5\text{-}C_5H_5)Cl_2]_2$ (100 mg, 0.21 mmol) was then added with stirring, and the mixture was stirred for 5 min at room temperature. The resulting black **1** was collected by filtration, washed with ethanol and hexane, and dried in vacuo (200 mg, 89%). $C_{13}H_9RhS_8$ (524.65): calcd. C 29.76, H 1.73; found C 29.60, H 1.89. ^{1}H NMR ([D$_6$]DMSO): δ = 3.41 (s, 5 H, CH_2), 5.97 (s, 5 H, C_5H_5) ppm.

Similarly, violet **2** was prepared by the reaction of an ethanol solution of $[NMe_4]_2[C_8H_4S_8]$ with a dichloromethane solution of $[Rh(\eta^5\text{-}C_5Me_5)Cl_2]_2$ (94% yield). $C_{18}H_{19}RhS_8$ (594.79): calcd. C 36.34, H 3.51; found C 36.35, H, 3.22. ^{1}H NMR (CD_2Cl_2): δ = 2.01 (s, 15 H, C_5Me_5), 3.27 (s, 4 H, CH_2) ppm.

Complex **3** was also prepared by the reaction of $[NMe_4]_2[C_8H_4S_8]$ with $[Ir(\eta^5\text{-}C_5Me_5)Cl_2]_2$ as a violet solid by the same procedure as described for **2** (94%). $C_{18}H_{19}IrS_8$ (684.10): calcd. C 31.60, H 2.80; found C 31.68, H 3.06. ^{1}H NMR (CD_2Cl_2): δ = 2.10 (s, 15 H, C_5Me_5), 3.28 (s, 4 H, CH_2) ppm.

Preparation of $[Rh(\eta^5\text{-}C_5H_5)(C_8H_4S_8)](Br)$ (4), $[RhBr(\eta^5\text{-}C_5Me_5)(C_8H_4S_8)]$ (5) and $[IrBr(\eta^5\text{-}C_5Me_5)(C_8H_4S_8)]$ (6): A dichloromethane (1.0 mL) solution of bromine [2.6 mm^3 (d = 3.1 g cm^{-3}), 0.050 mmol] was added with stirring to a dichloromethane (500 mL) solution of **1** (53 mg, 0.10 mmol), and the mixture was stirred for 15 h. The obtained black **4** was collected by filtration, washed with dichloromethane and hexane, and dried in vacuo (18 mg, 30%). $C_{13}H_9BrRhS_8$ (604.56): calcd. C 25.83, H 1.50; found C 25.26, H 1.76.

Similarly, the reaction of **2** (0.10 mmol) with bromine (0.05 mmol) in dichloromethane (100 mL) afforded black **5** (80%).

$C_{18}H_{19}BrRhS_8$ (674.69): calcd. C 32.04, H 2.84; found C 32.17, H 2.92. The presence of the Rh−Br bond in **5** was confirmed by ESR spectroscopy, as described above.

Complex **6** was also obtained by the reaction of **3** with bromine in dichloromethane as a black solid according to the procedure described for **4** (81%). $C_{18}H_{19}BrIrS_8$ (764.00): calcd. C 28.30, H 2.51; found C 27.71, H 2.70. The presence of the Ir−Br bond of **6** was confirmed by ESR spectroscopy, as described above.

Preparation of [Rh(η^5-C_5H_5)($C_8H_4S_8$)](I) (7) and [Rh(η^5-C_5H_5)($C_8H_4S_8$)]($I_{4.2}$) (8): A dichloromethane (10 mL) solution of iodine (6.3 mg, 0.025 mmol) was added with stirring to a dichloromethane (500 mL) solution of **1** (53 mg, 0.10 mmol) and the solution was stirred for 15 h. The obtained black **7** was collected by filtration, washed with dichloromethane and hexane, and dried in vacuo (12 mg, 19%). $C_{13}H_9IRhS_8$ (651.55): calcd. C 23.96, H 1.39; found C 24.28, H 1.50.

Similarly, black **8** was obtained from the reaction of **1** with 10 molar equivalents of iodine in dichloromethane (57%). $C_{13}H_9I_{4.2}RhS_8$ (1331.98): calcd. C 14.76, H 0.86; found C 14.56, H 0.96. The Raman spectrum of **8** showed that it contains both the I_3^- and I_5^- ions [114 cm^{-1} ν(I_3^-), 166 cm^{-1} ν(I_5^-)].[14,15]

Preparation of [RhI(η^5-C_5Me_5)($C_8H_4S_8$)] (9), [RhI(η^5-C_5Me_5)($C_8H_4S_8$)](I_3) (10), [IrI(η^5-C_5Me_5)($C_8H_4S_8$)] (11) and [IrI(η^5-C_5Me_5)($C_8H_4S_8$)](I_3) (12): A dichloromethane (100 mL) solution of **2** (60 mg, 0.10 mmol) was added with stirring to a dichloromethane (10 mL) solution of iodine (13 mg, 0.050 mmol) and the solution was stirred for 5 min. The volume of the solution was reduced to 50 mL under reduced pressure and hexane was added to the solution (500 mL) to afford black **9**. This was collected by filtration, washed with hexane, and dried in vacuo (60 mg, 83%). $C_{18}H_{19}IRhS_8$ (787.01): calcd. C 29.96, H 2.65; found C 29.19, H 2.66. The presence of the Rh−I bond of **9** was confirmed by ESR spectroscopy, as described below.

In a similar procedure, a dichloromethane (200 mL) solution of **2** (120 mg, 0.20 mmol) was added to a dichloromethane (40 mL) solution of iodine (100 mg, 0.40 mmol) to afford black **10** (170 mg, 77%). $C_{18}H_{19}I_4RhS_8$ (1363.67): calcd. C 19.61, H 1.74; found C 19.88, H 1.68. The presence of the I_3^- ion was confirmed by the Raman spectrum [112 cm^{-1} ν(I_3^-)]. Black plates of **10** suitable for X-ray crystallography were obtained by recrystallization from a dichloromethane (20 mL) solution of **2** (0.020 mmol) and iodine (0.030 mmol) upon addition of hexane (40 mL).

Complexes **11** and **12** were also obtained by reaction of **3** with iodine according to the procedures described for **9** and **10**, respectively, as black solids (65 and 70%, respectively). For **11**. $C_{18}H_{19}IIrS_8$ (811.00): calcd. C 26.30, H 2.51; found C 26.29, H, 2.51. For **12**. $C_{18}H_{19}I_4IrS_8$ (1191.70): calcd. C 18.14, H 1.61; found C 18.18, H 1.79. The Raman spectrum of **12** showed the presence of both the I_3^- and I_5^- ions [109 and 166 cm^{-1}, respectively]. Black plates of **12** suitable for X-ray crystallography were obtained by recrystallization from a dichloromethane (30 mL) solution of **12** (0.010 mmol) upon further addition of hexane (60 mL).

Preparation of [Rh(η^5-C_5Me_5)($C_8H_4S_8$)][PF_6] (13) and [Ir(η^5-C_5Me_5)($C_8H_4S_8$)][PF_6] (14): A dichloromethane (100 mL) solution of [Fe(η^5-C_5H_5)$_2$][PF_6] (33 mg, 0.10 mmol) was added with stirring to a dichloromethane (100 mL) solution of **2** (60 mg, 0.10 mmol). The volume of the solution was reduced to 50 mL under reduced pressure and then hexane (500 mL) was added, to yield black **13**. This was collected by filtration, washed with hexane, and dried in vacuo (60 mg, 81%). $C_{18}H_{19}F_6PRhS_8$ (739.75): calcd. C 29.23, H 2.59; found C 30.23, H 2.70.

By a similar procedure, a dichloromethane (200 mL) solution of **3** (68 mg, 0.10 mmol) was added to a dichloromethane (100 mL) solution of [Fe(η^5-C_5H_5)$_2$][PF_6] (33 mg, 0.10 mmol) to give black **14** (69 mg, 83%). $C_{18}H_{19}F_6IrPS_8$ (829.06): calcd. C 26.08, H 2.33; found C 26.78, H 2.55.

Physical Measurements: IR, electronic absorption, ESR[27] and powder reflectance spectra[12] were recorded as described previously. ^{1}H NMR spectra were also measured as reported previously.[28] Raman spectra were measured using a Nippon-bunko NR-1800 laser-Raman spectrophotometer at the Graduate School of Science, Osaka University. Cyclic voltammograms of the complexes in dichloromethane were measured using [NBu_4][ClO_4] as an electrolyte.[29] The electrical resistivities of the oxidized complexes were measured at room temperature for compacted pellets by the conventional two-probe method.[29]

Crystal-Structure Determinations of [RhI(η^5-C_5Me_5)($C_8H_4S_8$)](I_3) (10) and [IrI(η^5-C_5Me_5)($C_8H_4S_8$)](I_3) (12): Diffraction data were collected up to $2\theta = 60.0°$ for **10** and 55.0° for **12** on a Rigaku RAXIS-RAPID imaging plate diffractometer equipped with a Rigaku low-temperature device (liquid nitrogen as the coolant) and graphite-monochromated Mo-K_α ($\lambda = 0.71069$ Å) radiation at the Graduate School of Engineering, Osaka University. Indexing was performed for reflections obtained from three oscillations exposed for 200 s. The final values of the cell parameters were obtained from least-squares refinement of the positions of 32780 observed reflections for **10** and of 39553 reflections for **12**. Equivalent reflections were merged by use of the PROCESS-AUTO program package. For **10**, 25640 reflections were unique (R_{int} = 0.047) from 50511, and for **12** 19335 reflections were unique (R_{int} = 0.047) from 37695. The data were corrected for absorption using the program ABSCOR[30] (transmission factors: 0.475−0.900 for **10** and 0.322−0.634 for **12**) and for Lorentz and polarization effects. Crystallographic data are summarized in Table 3.

Table 3. Crystallographic data for [IrI(η^5-C_5Me_5)($C_8H_4S_8$)](I_3) (**10**) and [RhI(η^5-C_5Me_5)($C_8H_4S_8$)](I_3) (**12**)

	10	**12**
Empirical formula	$C_{18}H_{19}I_4RhS_8$	$C_{18}H_{19}I_4IrS_8$
M	1102.35	1191.67
Crystal system	triclinic	triclinic
Space group	$P\bar{1}$	$P\bar{1}$
Unit cell dimensions		
a (Å)	11.1432(3)	11.1666(3)
b (Å)	18.4541(3)	18.5094(6)
c (Å)	24.4044(5)	24.426(1)
α (°)	103.4506(4)	103.639(2)
β (°)	102.5416(7)	102.570(2)
γ (°)	105.552(1)	105.628(1)
V (Å^3)	4488.0(2)	4506.5(3)
Z	6	6
$D_{calcd.}$ (g cm^{-3})	2.447	2.634
T (K)	223	233
μ (Mo-K_α) (mm^{-1})	5.27	9.13
Reflection collected	50511	37695
Independent reflections	25640	19306
R[a]	0.042	0.052
R_w [b] (all data)	0.122[c]	0.125[d]

[a] $R = \Sigma(F_o^2 - F_c^2) / \Sigma F_o^2$. [b] $R_w = \Sigma w(F_o^2 - F_c^2)^2$. [c] $w^{-1} = \sigma^2(F_o^2) + (0.0601P)^2 + 0.0000P$. [d] $w^{-1} = \sigma^2(F_o^2) + (0.1000P)^2 + 0.0000P$, where $P = (F_o^2 + 2F_c^2)/3$.

The structure was solved by the Patterson method (PATTY),[31] expanded using Fourier techniques (DIRDIF94)[32] and refined on F^2 by the full-matrix least-squares method (SHELXL-97).[33] All the non-hydrogen atoms were refined anisotropically. The positions of all hydrogen atoms were calculated geometrically and refined with isotropic thermal parameters riding on those of the parent atoms. Atomic scattering factors were taken from the usual sources.[34] Figure 1 and 2 were drawn with ORTEP II.[35]
CCDC-219811 (for **10**) and -219812 (for **12**) contain the supplementary crystallographic data for this paper. These data can be obtained free of charge at www.ccdc.cam.au.uk/conts/retrieving.html [or from the Cambridge Crystallographic Data Centre, 12 Union Road, Cambridge CB2 1EZ, UK; Fax: (internat.) + 44-1223-336-033; E-mail: deposit@ccdc.cam.ac.uk].

Acknowledgments

We are grateful to Professor S. Suzuki (Graduate School of Science) for measurement of ESR spectra. This research was supported in part by grants-in-Aid for scientific research (nos. 14044056 and 15550049) from the Ministry of Education, Science, Sports and Culture, Japan, and by a Strategic Research Base Upbringing Special Coordination Fund for Promoting Science and Technology.

[1] P. Cassoux, L. Valade, K. Kobayashi, A. Kobayashi, R. A. Clark, A. E. Underhill, *Coord. Chem. Rev.* **1991**, *110*, 115−160.
[2] R.-M. Olk, B. Olk, W. Dietzsch, R. Kirmse, E. Hoyer, *Coord. Chem. Rev.* **1992**, *117*, 99−131.
[3] A. E. Pullen, R.-M. Olk, *Coord. Chem. Rev.* **1999**, *188*, 211−262.
[4] G. Matsubayashi, M. Nakano, H. Tamura, *Coord. Chem. Rev.* **2002**, *226*, 143−151.
[5] H. Mori, M. Nakano, H. Tamura, G. Matsubayashi, W. Mori, *Chem. Lett.* **1998**, 729−730.
[6] K. Kawabata, M. Nakano, H. Tamura, G. Matsubayashi, *J. Organomet. Chem.*, **2004**, *689*, 405−410.
[7] H. Mori, M. Nakano, H. Tamura, G. Matsubayashi, *J. Organomet. Chem.* **1999**, *574*, 77−85.
[8] K. Saito, M. Nakano, H. Tamura, G. Matsubayashi, *Inorg. Chem.* **2000**, *39*, 4815−4820.
[9] K. Saito, M. Nakano, H. Tamura, G. Matsubayashi, *J. Organomet. Chem.* **2001**, *625*, 7−17.
[10] M. Nakano, A. Kuroda, H. Tamura, R. Arakawa, G. Matsubayashi, *Inorg. Chim. Acta* **1998**, *279*, 165−171.
[11] G. Matsubayashi, M. Nakano, K. Saito, T. Yonamine, R. Arakawa, *J. Organomet. Chem.* **2000**, *611*, 364−369.
[12] T. Nakazono, M. Nakano, T. Tamura, G. Matsubayashi, *J. Mater. Chem.* **1999**, *9*, 2413−2417.
[13] K. Kawabata, M. Nakano, H. Tamura, G. Matsubayashi, manuscript to be published.
[14] M. Cowie, A. Gleizes, G. W. Grynkewich, D. W. Kalina, M. S. McClure, R. P. Scaringe, R. C. Teitelbaum, S. L. Ruby, J. A. Ibers, C. R. Kannewurf, T. J. Marks, *J. Am. Chem. Soc.* **1979**, *101*, 2921−2936.
[15] B. N. Diel, T. Inabe, J. W. Lyding, K. F. Schoch Jr., C. R. Kannewurf, T. J. Marks, *J. Am. Chem. Soc.* **1983**, *105*, 1551−1567.
[16] K. Kubo, M. Nakano, H. Tamura, G. Matsubayashi, M. Nakamoto, *J. Organomet. Chem.* **2003**, *669*, 141−148.
[17] R. Ziessel, M.-T. Youinou, F. Balegroune, D. Grandjean, *J. Organomet. Chem.* **1992**, *441*, 143−154.
[18] M.-J. Don, K. Yang, S. G. Bott, M. G. Richmond, *J. Organomet. Chem.* **1997**, *544*, 15−21.
[19] C.-H. Cheng, B. C. Spivack, R. Eisenberg, *J. Am. Chem. Soc.* **1977**, *99*, 3003−3011.
[20] K. Kubo, M. Nakano, H. Tamura, G. Matsubayashi, *Inorg. Chim. Acta* **2002**, *336*, 120− 124.
[21] K. Kubo, M. Nakano, H. Tamura, G. Matsubayashi, *Eur. J. Inorg. Chem.* **2003**, 4093−4098.
[22] J. W. Kang, K. Moseley, P. M. Maitlis, *J. Am. Chem. Soc.* **1969**, *91*, 5970−5977.
[23] "Jikken Kagaku Kouza (in Japanese)", Maruzen Co. Tokyo, Japan, **1991**, *18*, p. 344.
[24] N. Svenstrup, K. M. Rasmussen, T. K. Kansen, J. Becher, *Synthesis* **1994**, 809.
[25] L. Binet, J. M. Fabre, C. Montginoul, K. B. Simonsen, J. Becher, *J. Chem. Soc., Perkin Trans. 1* **1996**, 783−788.
[26] K. Akiba, G. Matsubayashi, T. Tanaka, *Inorg. Chim. Acta* **1989**, *165*, 245−248.
[27] K. Natsuaki, M. Nakano, G. Matsubayashi, *Inorg. Chim. Acta* **2000**, *299*, 112−117.
[28] G. Matsubayashi, T. Ryowa, H. Tamura, M. Nakano, R. Arakawa, *J. Organomet. Chem.* **2002**, *645*, 94−100.
[29] A. Nakahama, M. Nakano, G. Matsubayashi, *Inorg. Chim. Acta* **1999**, *284*, 55−60.
[30] T. Higashi, ABSCOR, a computer program for absorption correction, Rigaku Corporation, Tokyo, Japan, **1995**.
[31] PATTY: P. T. Beurskens, G. Admiraal, G. Beurskens, W. P. Bosman, R. de Gelder, R. Israel, J. M. M. Smits, DIRDIF94 program system, Technical report of the Crystallography laboratory, University of Nijmegen, The Netherlands, **1994**.
[32] P. T. Beurskens, G. Admiraal, G. Beurskens, W. P. Bosman, R. de Gelder, R. Israel, J. M. M. Smits, DIRDIF94 program system, Technical report of the Crystallography Laboratory, University of Nijmegen, The Netherlands, **1994**.
[33] G. M. Sheldrick, SHELXL 97, a computer program for the refinement of crystal structures, University of Göttingen, Germany, **1997**.
[34] *International Tables for X-ray Crystallography*, vol. 4, Kynoch Press, Birmingham, England, **1974**.
[35] C. K. Johnson, ORTEP-II, Report ORNL-5138, Oak Ridge National Laboratory, Oak Ridge, TN, **1976**.

Received October 23, 2003
Early View Article
Published Online April 1, 2004

